# The Telescope Array experiment

## The largest cosmic ray detector array in the Northern Hemisphere

Armando di Matteo*
armando.di.matteo@ulb.ac.be

Service de Physique Théorique
Université Libre de Bruxelles (ULB)
Brussels, Belgium

Kick-off meeting, COST Action CA18108 (QG-MM)
2–4 October 2019
Barcelona, Spain

*Now at INFN Torino, Turin, Italy

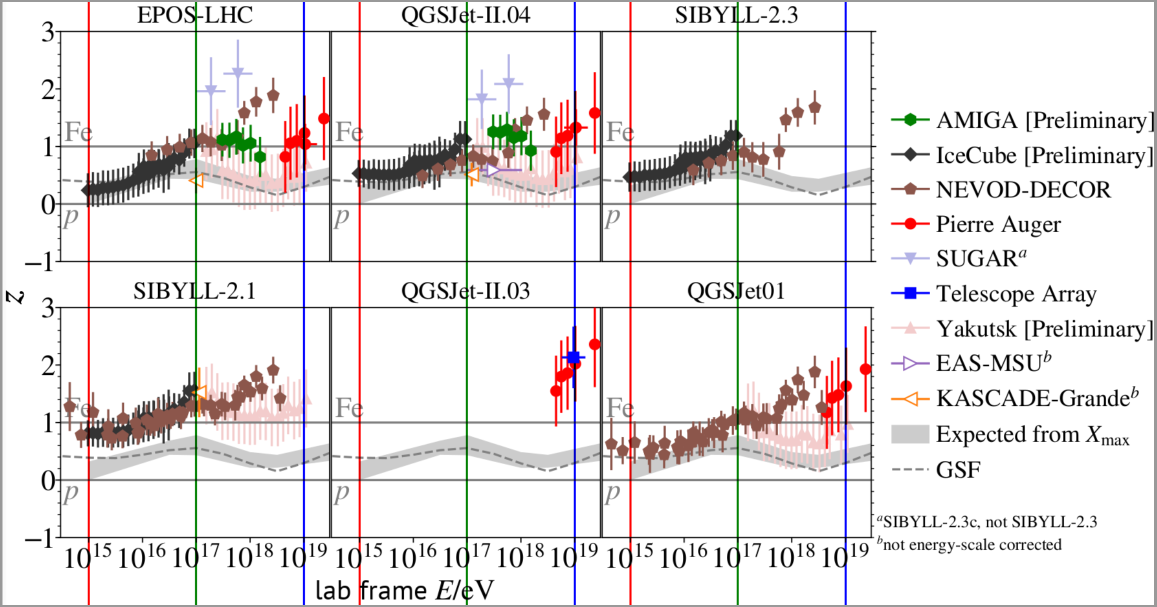


$\sqrt{s_{\text{protons at 1st interaction}}}$ = 1.4 TeV = 0.1LHC, 14 TeV = LHC, 140 TeV = 10LHC

# The Telescope Array experiment

## The largest cosmic ray detector array in the Northern Hemisphere

Armando di Matteo†
armando.di.matteo@ulb.ac.be

Service de Physique Théorique
Université Libre de Bruxelles (ULB)
Brussels, Belgium

Kick-off meeting, COST Action CA18108 (QG-MM)
2–4 October 2019
Barcelona, Spain

† Now at INFN Torino, Turin, Italy

# The Telescope Array collaboration

## 147 members, 36 institutions, 6 countries

R.U. Abbasi[1], M. Abe[2], T. Abu-Zayyad[1], M. Allen[1], R. Azuma[3], E. Barcikowski[1], J.W. Belz[1], D.R. Bergman[1], S.A. Blake[1], R. Cady[1], B.G. Cheon[4], J. Chiba[5], M. Chikawa[6], **A. di Matteo**[7]*, T. Fujii[8], K. Fujita[9], R. Fujiwara[9], M. Fukushima[10,11], G. Furlich[1], W. Hanlon[1], M. Hayashi[12], Y. Hayashi[9], N. Hayashida[13], K. Hibino[13], K. Honda[14], D. Ikeda[15], T. Inadomi[16], N. Inoue[2], T. Ishii[14], R. Ishimori[3], H. Ito[17], D. Ivanov[1], H. Iwakura[16], H.M. Jeong[18], S. Jeong[18], C.C.H. Jui[1], K. Kadota[19], F. Kakimoto[3], O. Kalashev[20], K. Kasahara[21], S. Kasami[22], H. Kawai[23], S. Kawakami[9], S. Kawana[2], K. Kawata[10], E. Kido[10], H.B. Kim[4], J.H. Kim[1], J.H. Kim[9], S. Kishigami[9], V. Kuzmin[20]†, M. Kuznetsov[7,20], Y.J. Kwon[24], K.H. Lee[18], B. Lubsandorzhiev[20], J.P. Lundquist[1], K. Machida[14], K. Martens[11], H. Matsumiya[9], T. Matsuyama[9], J.N. Matthews[1], R. Mayta[9], M. Minamino[9], K. Mukai[14], I. Myers[1], S. Nagataki[17], K. Nakai[9], R. Nakamura[16], T. Nakamura[25], Y. Nakamura[16], T. Nonaka[10], H. Oda[9], S. Ogio[9,26], M. Ohnishi[10], H. Ohoka[10], Y. Oku[22], T. Okuda[27], Y. Omura[9], M. Ono[17], R. Onogi[9], A. Oshima[9], S. Ozawa[21], I.H. Park[18], M.S. Pshirkov[20,28], J. Remington[1], D.C. Rodriguez[1], G. Rubtsov[20], D. Ryu[29], H. Sagawa[10], R. Sahara[9], K. Saito[10], Y. Saito[16], N. Sakaki[10], T. Sako[10], N. Sakurai[9], K. Sano[16], L.M. Scott[30], T. Seki[16], K. Sekino[10], P.D. Shah[1], F. Shibata[14], T. Shibata[10], H. Shimodaira[10], B.K. Shin[9], H.S. Shin[10], J.D. Smith[1], P. Sokolsky[1], N. Sone[16], B.T. Stokes[1], S.R. Stratton[1,30], T.A. Stroman[1], T. Suzawa[2], Y. Takagi[9], Y. Takahashi[9], M. Takamura[5], M. Takeda[10], R. Takeishi[18], A. Taketa[15], M. Takita[10], Y. Tameda[22], H. Tanaka[9], K. Tanaka[31], M. Tanaka[32], Y. Tanoue[9], S.B. Thomas[1], G.B. Thomson[1], P. Tinyakov[7,20], I. Tkachev[20], H. Tokuno[3], T. Tomida[16], S. Troitsky[20], Y. Tsunesada[9,26], Y. Uchihori[33], S. Udo[13], T. Uehama[16], F. Urban[34], T. Wong[1], M. Yamamoto[16], H. Yamaoka[32], K. Yamazaki[13], J. Yang[35], K. Yashiro[5], M. Yosei[22], H. Yoshii[36], Y. Nakamura[16], Y. Zhezher[20], and Z. Zundel[1]

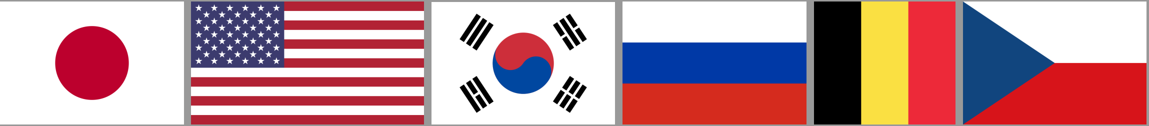

*Currently at INFN, sezione di Torino, Turin, Italy

†Deceased

# Outline

1. The detectors
2. Event reconstruction
3. Results

# Location


39.3° N, 112.9° W, 1400 m a.s.l.

Millard County, Utah, USA

Semi-desert area 200 km SW of SLC

green, magenta original

blue, red new additions

yellow under construction

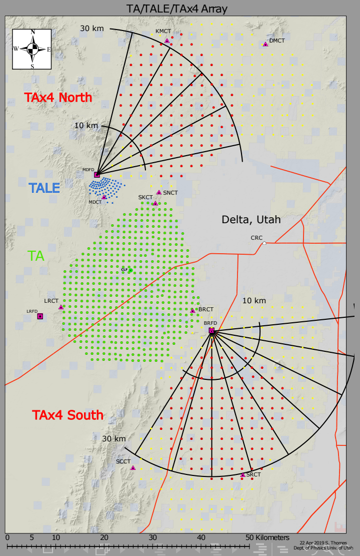

# The original surface detector (SD) array

(deployed in 2006–2008)

TA collab., *Nucl. Instrum. Meth.* **A689** (2012) 87 [1201.4964]

94.5% duty cycle

- 507 detectors in a 1.2 km square grid (700 $km^2$ total)
- $\sim$ 100% efficient for $E \geq 10^{19}$ eV, $\theta < 45°$

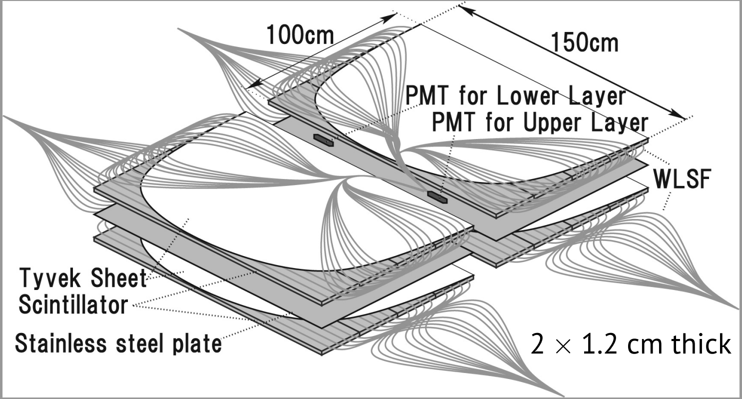


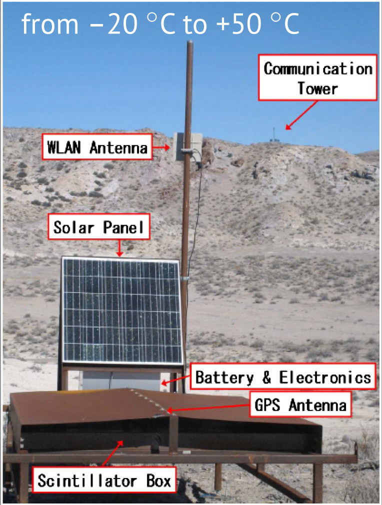

# The original Middle Drum fluorescence detector (deployed in 2006–2007)

TA collab., *Astropart. Phys.* **39** (2012) 109 [1202.5141]

- 14 telescopes refurbished from the HiRes-1 experiment (1997–2006), each with: a 5.2 $m^2$ mirror, 256 PMTs using sample-and-hold electronics, $17^\circ \times 14^\circ$ FoV
- Overall FoV: $112^\circ$ in azimuth, elevations from $3^\circ$ to $31^\circ$


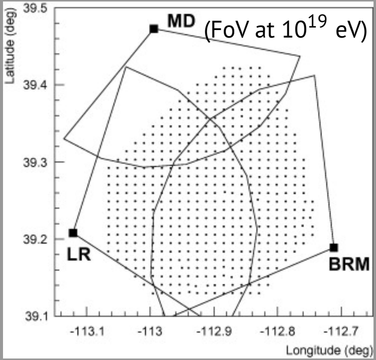

# The Black Rock Mesa and Long Ridge fluorescence detectors

TA collab., *Nucl. Instrum. Meth.* **676** (2012) 54 [1201.0002] 11.0% and 9.0% duty cycles

- 12 telescopes newly designed for TA at each site, each with:
  a 6.8 $m^2$ mirror, 256 PMTs using flash analog-to-digital converters, $18^\circ \times 15.5^\circ$ FoV
- Overall FoV: $108^\circ$ in azimuth, elevations from $3^\circ$ to $33^\circ$

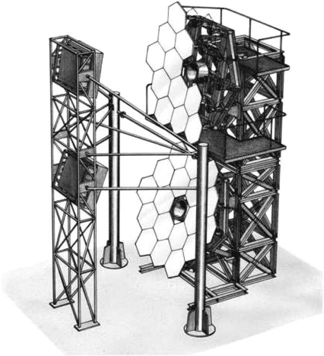

# The Telescope Array Low-energy Extension (TALE)

TA collab., PoS (ICRC2019) 375 and references therein

## Fluorescence detector (deployed in 2012–2013)

- 10 telescopes at Middle Drum, refurbished from HiRes
- Covers 114° in azimuth and elevations from 30° to 57°

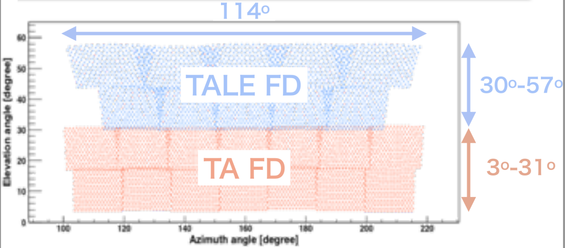


## Surface detector (deployed in 2018)

- 40 SDs with 400 m spacing
- 40 SDs with 600 m spacing
- 23 SDs with 1.2 km spacing (planned)

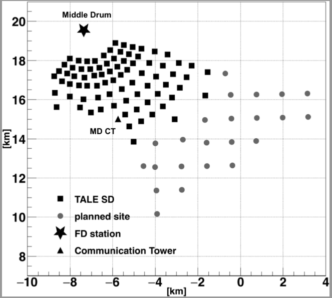

# TA$\times$4

TA collab., PoS (ICRC2019) 312 and references therein

## Surface detectors

- 257 SDs on a 2.08 km square grid (deployed in Feb–Mar 2019)
- 243 more to be deployed

- Total area (TA + TA$\times$4): 3 000 km$^2$
- $> 95\%$ efficiency for $E > 57$ EeV

## Fluorescence detectors

- 4 more telescopes at Middle Drum, looking north (first light in Feb 2018)

- 8 more telescopes at Black Rock Mesa, looking south (under construction)

# Outline

# FD event reconstruction

TA collab., *Astropart. Phys.* **61** (2015) 93 [1305.7273]

- Shower geometry fitted to signal timings (stereo > hybrid > monocular)
- Air fluorescence yield from Kakimoto et al.
- Shower profile fitted by Gaisser–Hillas function: $N(X|N_{max}, \lambda, X_0, X_{max}) =$
  $$N_{max}\left(\frac{X-X_0}{X_{max}-X_0}\right)^{\frac{X_{max}-X_0}{\lambda}}\exp\left(\frac{X_{max}-X}{\lambda}\right),$$ where
  - $X$: atmospheric depth $X = \int_{+\infty}^{z} \rho_{air}(h)\sec\theta\, dh$
  - $N_{max}$: normalization
  - $\lambda$: shape parameter
  - $X_0$: $X$ at first interaction
  - $X_{max}$: $X$ at shower maximum
- Calorimetric energy estimated as $\int_0^{+\infty} N(X)\, dX$
- Invisible energy estimated via parametrization from QGSJet II-03 proton simulations (7–9%)

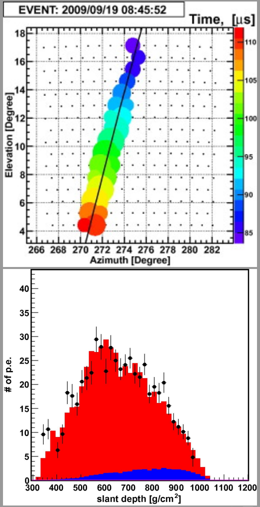


Systematics: $E$ ±21%
$X_{max}$ ±17 g/cm$^2$

Resolution:
$E$ 17% (mon.), 7% (hyb.)
$\hat{\mathbf{n}}$ 8° (mon.), 0.9° (hyb.)
$X_{max}$ 72 g/cm$^2$ (mon.), ~ 20 g/cm$^2$ (hyb.)

↙ Shower profile
**red**: fluorescence (domin. at $E \gtrsim 10^{17.3}$ eV)
**blue**: Cherenkov (domin. at $E \lesssim 10^{17.3}$ eV)

# SD event reconstruction

TA collab., *Astrophys. J.* **768** (2013) L1 [1205.5067] Resolution: $E < 20\%$, $\hat{\mathbf{n}} \sim 1.5^\circ$

- Shower geometry from fit of signal times to modified Linsley shower-shape function
- Lateral distribution profile fitted by $\rho(r|\rho_0,\eta) = \rho_0(r/R_M)^{1.2}(1 + r/R_M)^{1.2-\eta}(1 + (r/\mathrm{km})^2)^{-0.6}$ ($r$: distance from shower axis, $\rho_0$: normalization, $R_M$: Molière radius of air) and evaluated at $r = 800$ m
- $E_{SD}$ estimated from $(S_{800}, \theta)$ via a look-up table from QGSJet II-03 proton simulations
  - Constant intensity cuts (as used by Auger) found to return same $E_{SD}$ to within $\sim 3\%$
- $E_{SD}$ /= 1.27 in order to bring average $E_{SD}$ and $E_{FD}$ of hybrid events into agreement

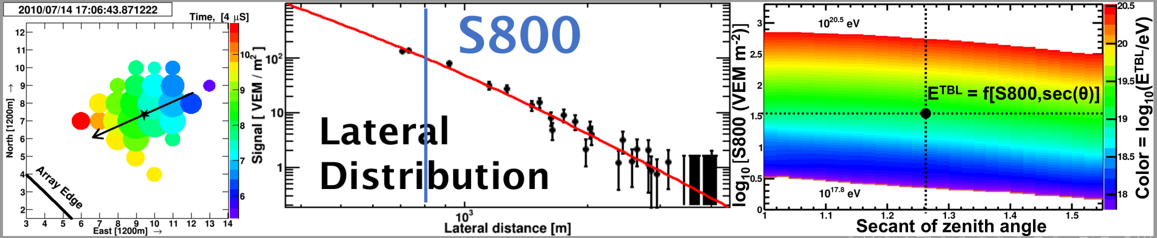

# Outline

# Energy spectrum

TA collab., PoS (ICRC2019) 298 and references therein

## TALE FD

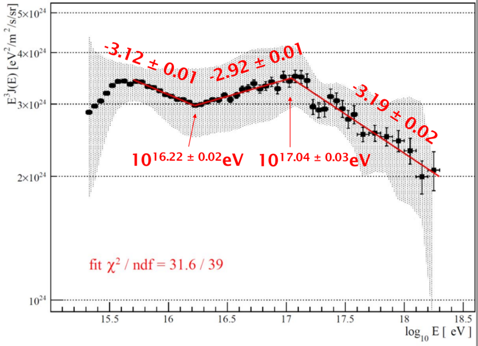


## TA SD

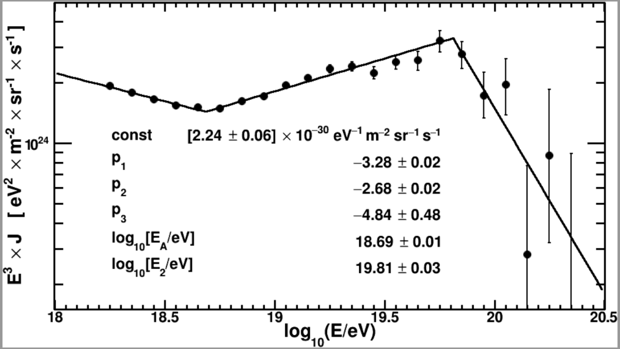

# Combined spectrum

(Note: no artificial rescaling of energies or exposures)

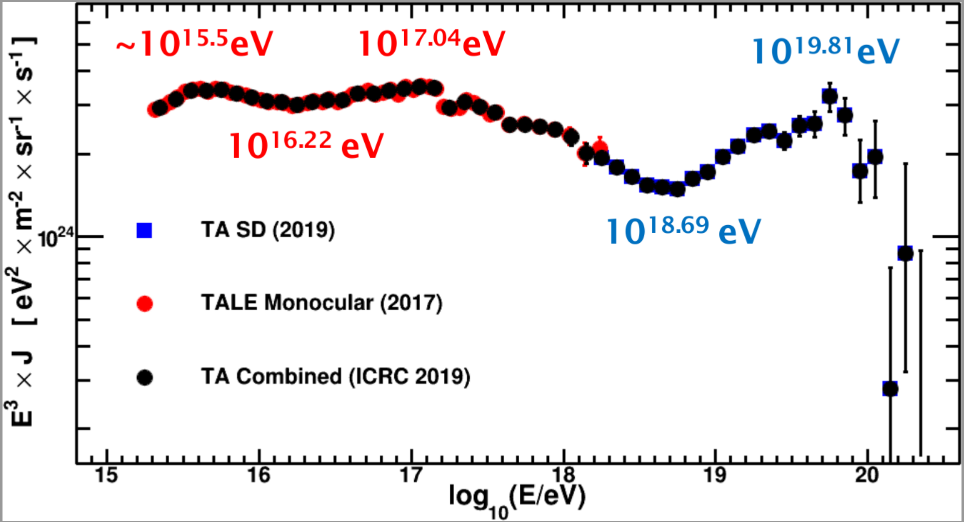

# Declination dependence of UHE spectrum

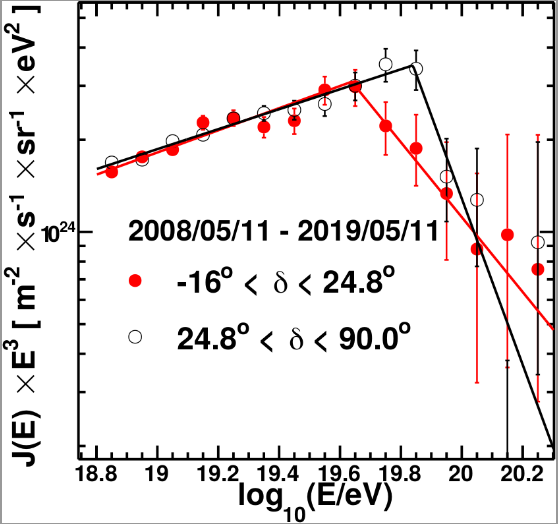


- Overlap with Auger $\theta < 60^\circ$ FoV:
  - Break at $10^{19.64\pm0.04}$ eV

  (spectrum still not quite the same as Auger's – but much closer, and break point energies do agree)
- Rest of the sky:
  - Break at $10^{19.84\pm0.02}$ eV

Post-trial significance of difference: $4.3\sigma$

# Mass composition (stereo FD)

TA collab., PoS (ICRC2019) 191 and references therein

**red**, **blue** QGSJet II-04 simulations with detection biases taken into account

Systematic uncertainty on data: $\pm 15$ g/cm$^2$

Resolution: $< 25$ g/cm$^2$

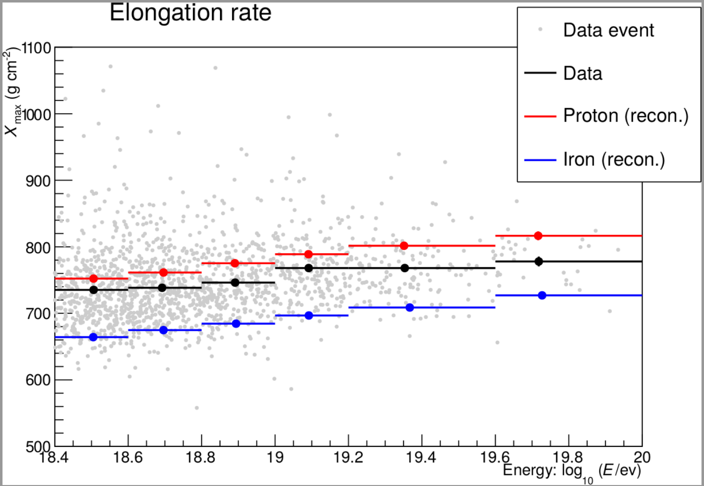

# Mass composition (Black Rock Mesa + Long Ridge hybrid) — I

TA collab., PoS (ICRC2019) 280 and references therein

- $X_{max}$ distribution predicted by QGSJet II-04, but allowed to be shifted to take into account model uncertainty (and measurement systematics)

## Single elements

($10^{18.4}$–$10^{18.5}$ eV)

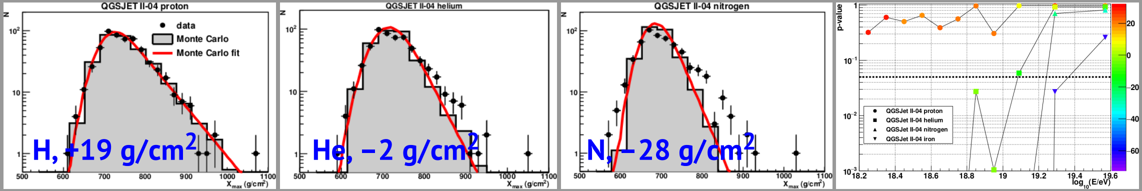


$E < 10^{18.8}$ eV: Any pure element other than H excluded at $p < 10^{-3}$
$E < 10^{19.2}$ eV: Pure elements other than H or He excluded at $p < 10^{-3}$
$E \geq 10^{19.4}$ eV: Not enough data (19 events) to exclude anything from H to Fe at $p < 5\%$

# Mass composition (Black Rock Mesa + Long Ridge hybrid) — II

TA collab., PoS (ICRC2019) 280 and references therein

## Two-element mixes $(10^{18.2}–10^{19.1}$ eV$)$

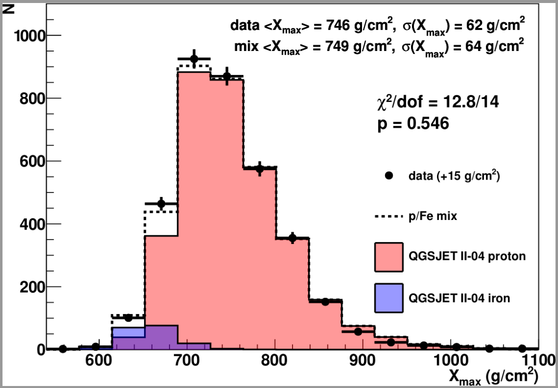


- Compatible with 95% p + 5% Fe

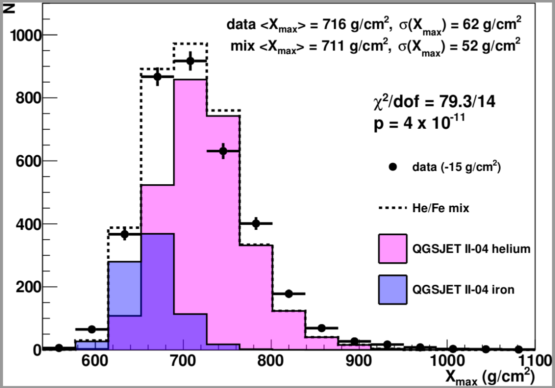


- Not compatible with any He + Fe mixes

# Mass composition (Black Rock Mesa + Long Ridge hybrid) — III

TA collab., PoS (ICRC2019) 280 and references therein

## Four-element mixes $(10^{18.2}$–$10^{19.1}$ eV)

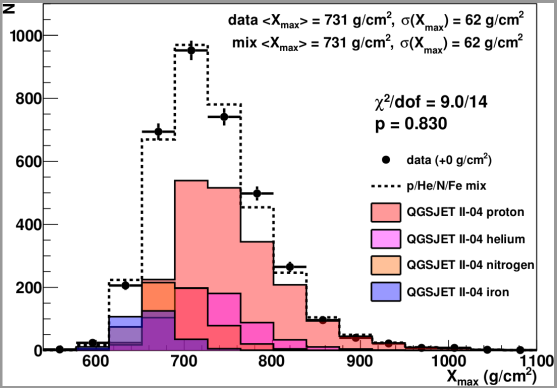


- 57% + 18% + 17% + 8% (no shift needed)

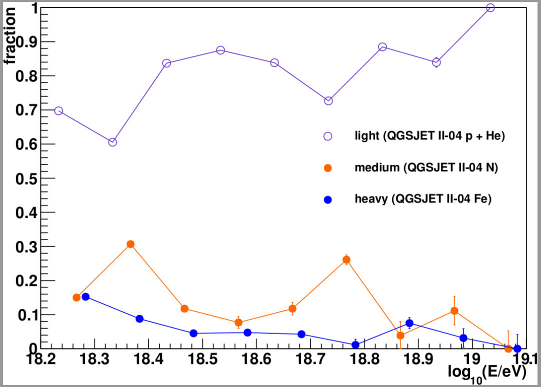


- No significant energy dependence

# Mass composition (SD array)

TA collab., *Phys. Rev.* **D99** (2019) 022002 [1808.03680]

- Boosted decision tree using 14 observables, trained on QGSJet II-03 simulations

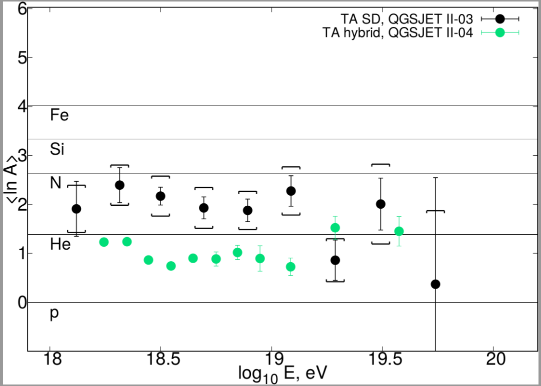


- Result: $\langle \ln A \rangle = 2.0 \pm 0.1_{\mathrm{stat}} \pm 0.4_{\mathrm{syst}}$; no significant $E$ dependence
- Can be improved used deep learning, see PoS (ICRC2019) 304.

# Limits on diffuse photon fluxes

TA collab., *Astropart. Phys.* **110** (2019) 8 [1811.03920]

- Boosted decision tree using 16 observables, trained on EGS4 and QGSJet II-03 simulations

| | $E_0$, eV | | | | |
|---|---|---|---|---|---|
| | $10^{18.0}$ | $10^{18.5}$ | $10^{19.0}$ | $10^{19.5}$ | $10^{20.0}$ |
| $\gamma$ candidates | 1 | 0 | 0 | 0 | 1 |
| $b$ | 0.55 | 1.01 | 0.97 | 0.80 | 0.49 |
| $\bar{n}$ < | 5.14 | 3.09 | 3.09 | 3.09 | 5.14 |
| $A_{eff}$ | 77 | 255 | 852 | 2351 | 4055 |
| $F_\gamma$ < | 0.067 | 0.012 | 0.0036 | 0.0013 | 0.0013 |

TABLE II. 95% CL upper limits on the number of photons in the data set $\bar{n}_\gamma$ and on the photon flux $F_\gamma$ ($\mathrm{km^{-2}yr^{-1}sr^{-1}}$). $b$ is an expected number of background photon candidates obtained with proton MC.

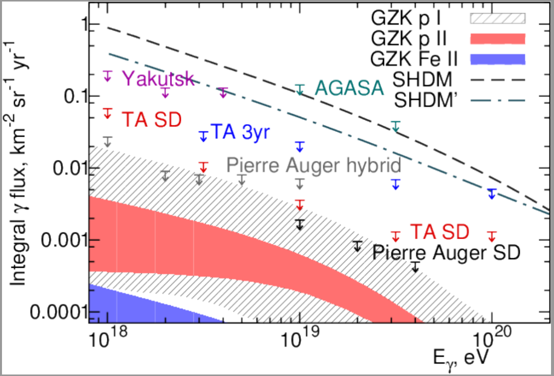

# Hotspot above 57 EeV

TA collab., *ApJL* **790** (2014) L21 [1404.5890]; PoS (ICRC2019) 310

Published, using 5 years of SD data

- $20^\circ$ radius around $(146.7^\circ, +43.2^\circ)$
- 19 events in the circle (72 total), 4.49 expected
- $5.1\sigma$ pre-trial $\rightarrow$ $3.4\sigma$ post-trial

Preliminary update, using 11 years

- $25^\circ$ radius around $(144.3^\circ, +40.3^\circ)$
- $5.1\sigma$ pre-trial $\rightarrow$ $2.9\sigma$ post-trial

(Loosened quality cuts, $\theta < 55^\circ$)

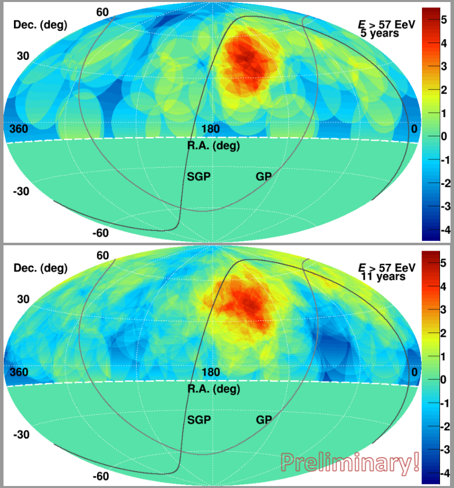

# Energy spectrum anisotropy

TA collab., *ApJ* **862** (2018) 91 [1802.05003]

- Coldspot in the same direction as the hotspot, but at lower $E$ ($10^{19.2}$–$10^{19.75}$ eV)

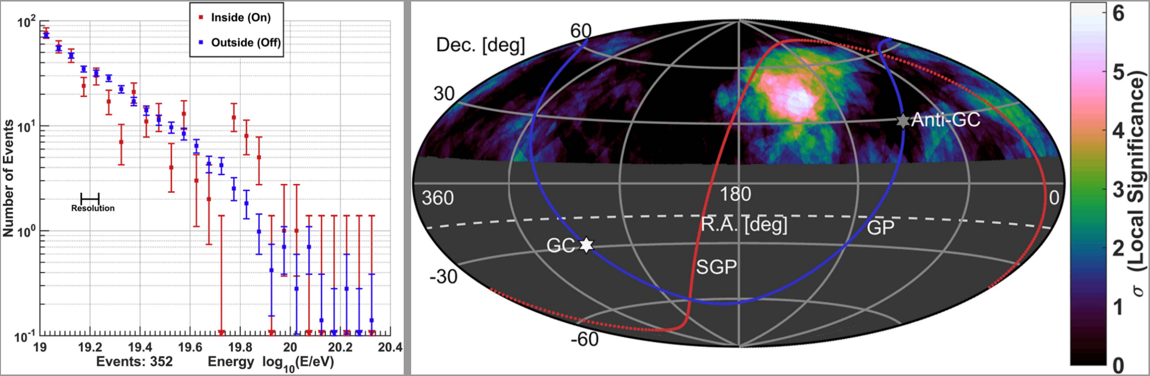


- $6.2\sigma$ pre-trial $\rightarrow$ $3.7\sigma$ post-trial

# Correlation with starburst galaxies (or lack thereof)

TA collab., *ApJL* **867** (2018) L27 [1809.01573]

- Auger arrival directions $\geq$ 39 EeV reported to correlate with a catalog of nearby SBGs (best fit: $\Psi$ = 12.9°, $f_{SBG}$ = 9.7%; 4.0$\sigma$ post-trial over isotropy, 3.0$\sigma$ over the overall galaxy distribution)
- North polar cap (incl. e.g. M82) outside the Auger field of view $\rightarrow$ TA replication interesting

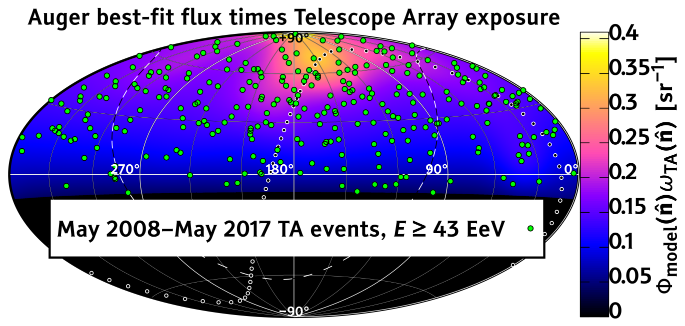


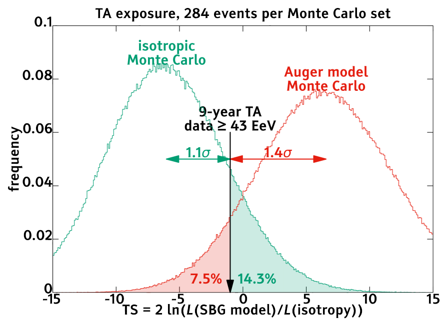


… but not (yet) enough data for that.

# Magnetic multiplets (preliminary) – I

TA collab., PoS (ICRC2019) 343

- Regular + random magnetic fields

→ Wedges in which energy anticorrelates with distance from the vertex (assuming same electric charge)

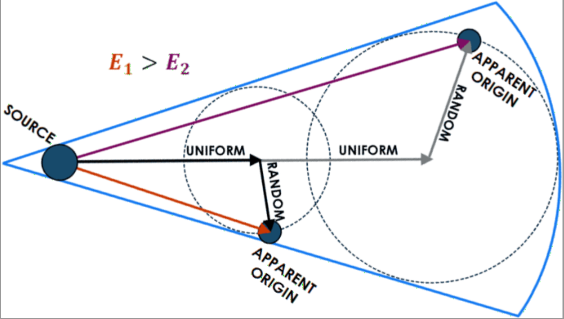


- For each vertex position, we scan over:
  - energy thresholds;
  - wedge lengths;
  - wedge widths;
  - wedge orientations;

for the most significant anticorrelation (using Kendall's $\tau_b$ rank correlation coefficient, unaffected by monotonic transformations).

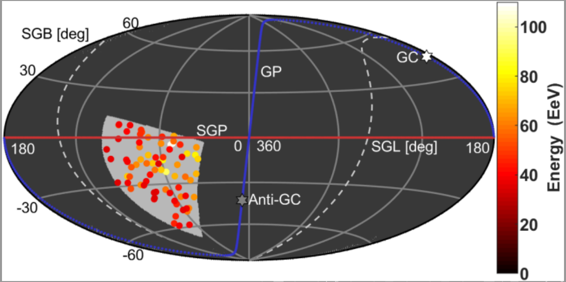

# Magnetic multiplets (preliminary) – II

TA collab., PoS (ICRC2019) 343

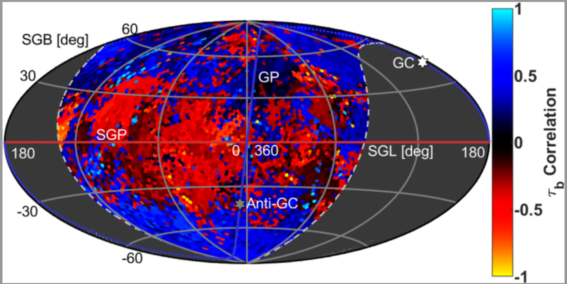


- Stronger anticorrelations near the supergalactic plane (∼ $4\sigma$ post-trial significance)

- Fit of $\Delta\theta$ vs $1/E \to$ estimate of $B$

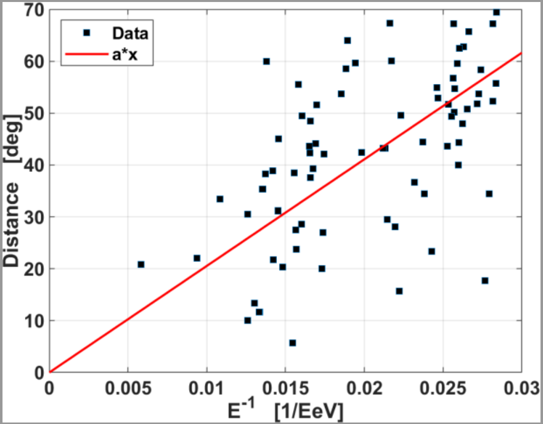


Here: $B = 12(ZD/3.7\text{ Mpc})^{-1}$ nG

# Magnetic multiplets (**very** preliminary) — III

https://www.icrc2019.org/uploads/1/1/9/0/119067782/lundquist_icrc2019.pdf

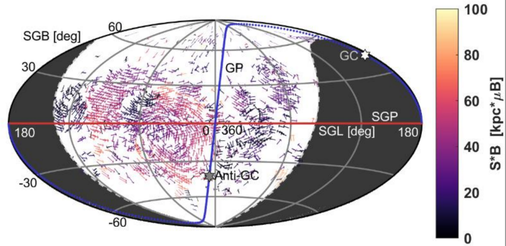


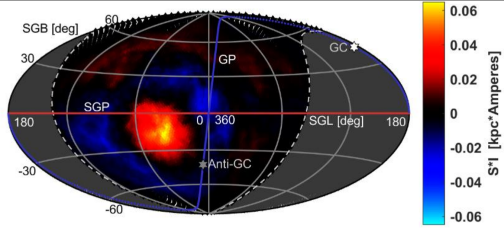


← Transverse **B** estimated at each grid point:
- Strength as in previous slide
- Direction 90° clockwise of wedge orientation

← Electric current density **toward**/**away from** us estimated as $\nabla \times \mathbf{B}/\mu_0$
(i.e., neglecting $\epsilon_0 \partial \mathbf{E}/\partial t$)

# Thanks for your attention!

# Outline

4 Back-up slides
- Test of systematics in declination dependence
- Auger vs TA spectrum in the common declination band
- Auger vs TA composition
- Time dependence of hotspot

# Test of systematics in declination dependence

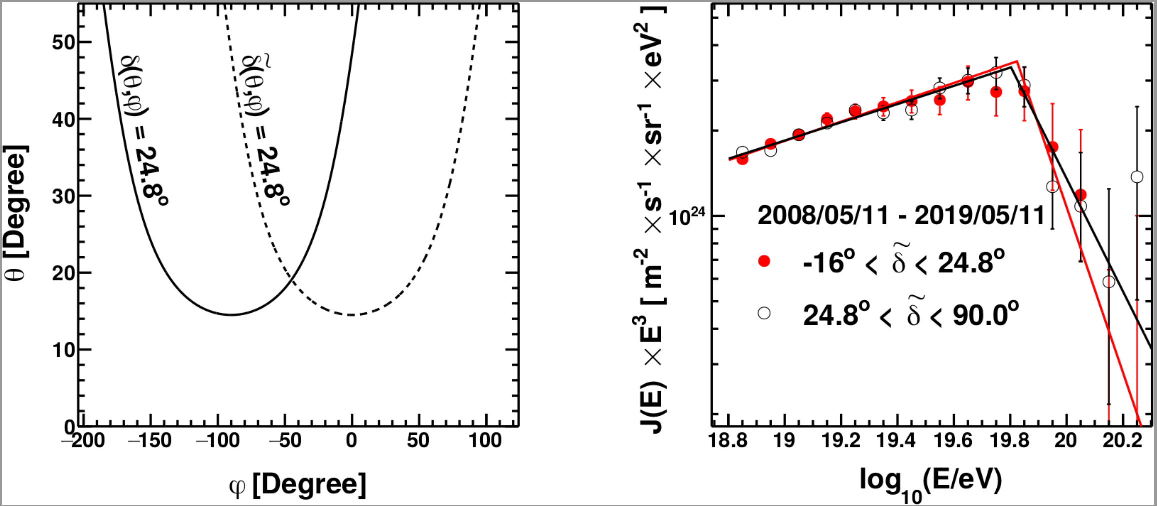

# Auger vs TA spectrum in the common declination band

Auger and TA collabs., PoS (ICRC2019) 234

| Data set | Difference between adjacent data sets |
|---|---|
| TA, north | |
| | large diff., PoS (ICRC2019) 298 (sl. 16) |
| TA, equat. | |
| | small diff., PoS (ICRC2019) 234 → |
| Auger + 11%, equat. | |
| | no diff., PoS (ICRC2017) 486 (prev. talk) |
| Auger + 11%, south | |

“south” = [−90°, −15°], “equat.” = (−15°, +25°), “north” = [+25°, +90°]

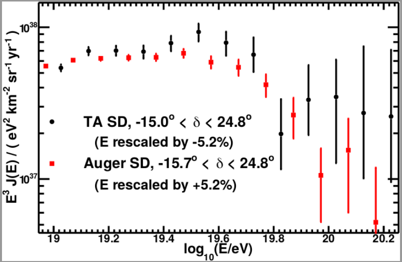


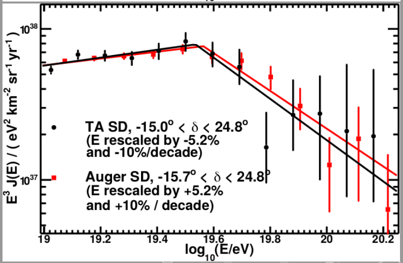


Note: $1/\omega(\delta)$ weights used to correct for possible declination dependence within each band

(see Auger+TA, *JPS Conf. Proc.* **19** (2018) 011020 for details)

# Auger vs TA composition

Auger and TA collabs., *EPJ Web Conf.* **210** (2019) 01009 [1905.06245]

## Black Rock Mesa and Long Ridge

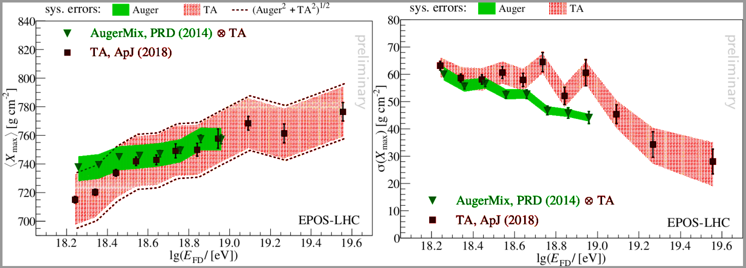


## Middle Drum

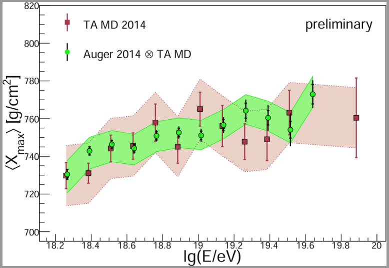


- Detector biases usually folded into simulations by TA and out of measurements by Auger

→ non-trivial comparisons (we had to fold TA biases into Auger measurements)

# Time dependence of hotspot

TA collab., PoS (ICRC2019) 310

- Variations well within expected Poisson fluctuations